Free-electron gas in the Apollonian network: Multifractal energy spectrum and its thermodynamic fingerprints

I. N. de Oliveira,[1] F. A. B. F. de Moura,[1] M. L. Lyra,[1] J. S. Andrade, Jr.,[2,4] and E. L. Albuquerque[3,4]
[1]*Instituto de Física, Universidade Federal de Alagoas, 57072-970 Maceió-AL, Brazil*
[2]*Departamento de Física, Universidade Federal do Ceará, 60451-970 Fortaleza-CE, Brazil*
[3]*Departamento de Física, Universidade Federal do Rio Grande do Norte, 59072-970 Natal-RN, Brazil*
[4]*Computational Physics for Engineering Materials, IfB, ETH-Zürich, CH-8093 Zürich, Switzerland*
(Received 6 October 2008; published 8 January 2009)

We study the free-electron gas in an Apollonian network within the tight-binding framework. The scale-free and small-world character of the underlying lattice is known to result in a quite structured energy spectrum with deltalike singularities, gaps, and minibands. After an exact numerical diagonalization of the corresponding adjacency matrix of the network with a finite number of generations, we employ a scaling analysis of the moments of the density of states to characterize its multifractality and report the associated singularity spectrum. The fractal nature of the energy spectrum is also shown to be reflected in the thermodynamic behavior by logarithmic modulations on the temperature dependence of the specific heat. The absence of chiral symmetry of the Apollonian network leads to distinct thermodynamic behaviors due to electrons and holes thermal excitations.

DOI: 10.1103/PhysRevE.79.016104 PACS number(s): 89.75.Hc, 64.60.aq, 05.30.Fk, 64.60.al

I. INTRODUCTION

The understanding of the physical and geometrical properties of deterministic nonperiodic systems has substantially increased after the discovery of quasicrystals in 1984 [1]. An appealing motivation for studying these kinds of structures was that they exhibit a highly fragmented energy spectrum displaying a self-similar pattern. From a strictly mathematical perspective, it has been proven that their spectra are *Cantor sets* in the thermodynamic limit [2]. The origin of this fractality can be attributed to the long-range order induced by the nonusual hierarchical structure of the quasiperiodic sequences used in the construction of the system [3,4]. While periodic potentials lead to continuous spectra and extended eigenvalues (Bloch-type energies), and random potentials lead to pure point spectra and exponentially localized states (the energy of the spectrum itself is always a regular object, with at most a finite number of bands), quasiperiodic Fibonacci-type potentials may lead to a Cantor set of zero (Lebesgue) measure energy spectrum, with neither extended nor localized eigenstates (for a review see Ref. [5]).

In recent years, extensive scientific work has been dedicated to the study of complex networks [6]. These structures with entirely novel topological properties have been very useful as realistic substrates for many different transport and information phenomena in a rich variety of social, biological, and physical systems [7–12]. In particular, much attention has been devoted to the study of networks with small-world and/or scale-free properties. The first case refers to structures where the diameter or average shortest path ℓ increases logarithmically with system size N (number of nodes), $\ell \sim \log N$, while the second corresponds to networks where the distribution of connectivity follows a power law, $p(k) \sim k^{-\gamma}$, with a characteristic exponent γ and k being the degree (connectivity) of the nodes.

When applied to the modeling of real materials, an obvious concern related to the feasibility of scale-free network models is whether or not they can be embedded in regular Euclidean lattices [13]. This feature is specially relevant in materials science and condensed matter physics. The small-world and scale-freeness characteristics found for some complex networks represent intriguing aspects of these structures. These characteristics are strongly related to anomalies found in their diffusional and electronic transport phenomena behavior [14,15]. From a slightly different viewpoint, the design of a suitable complex network to perform a specific task as a material or an engineering device or system might imply that the interplay between topology and dynamics in these structures should be a very important issue. In this way, deterministic networks are ideal candidates, since they are somehow controllable and can therefore be subjected to the particular constraints of the problem. However, the deterministic models for scale-free and/or small-world networks proposed in previous works [16,17] cannot be embedded in Euclidian space. Apollonian networks, on the other hand, are a particular class of deterministic networks that are scale-free, display small-world effect, can be embedded in a Euclidean lattice, and show space-filling as well as matching graph properties [18–20].

Although some studies have been made about the topological features of Apollonian networks and their effect on the behavior of a variety of transport and growth models [21–23], the connection between the hierarchical nature of the network and thermodynamic properties has not been deeply explored. Simplified fractals based on the triadic Cantor set [24,25], as well as on the critical attractor of the logistic and circle maps [26–28], have been recently used to model the energy spectrum of fractal/multifractal systems. More sophisticated methods, based on the spectrum of eigenvalues of Hamiltonian systems, were also proposed, looking for connections with several aspects of these spectra (scaling laws, fractal dimension, etc.) as well as for some kind of common behavior in the specific heat spectra. It has been shown, among other features, that the low-temperature spe-

cific heat behavior is intimately connected with some underlying fractal dimension characterizing the energy spectrum [29,30].

In this paper, we intend to investigate the thermodynamic behavior of a free electron gas distributed in an Apollonian network. Specifically, we will calculate the density of states (DOS) in the tight-binding approximation for one electron restricted to hop between the connected sites of an Apollonian network. We will employ a scaling analysis of the DOS to characterize its multifractal singularity spectrum. Further, we will explore the thermodynamic fingerprints of the underlying multifractal energy spectrum, in particular the anomalies appearing in the temperature dependence of the specific heat. We will provide a detailed analysis of the relation between the presence of logarithmic oscillations in the low-temperature specific heat and the level structure around the Fermi energy as a function of the band filling. The possible asymmetry between electrons and holes will also be explored in connection to the absence of chiral symmetry of the Apollonian network.

The plan of this work is as follows: in Sec. II, we present the one-particle Hamiltonian and the electronic density of states of the Apollonian network, using a theoretical model based on the Schrödinger equation in the tight-binding approximation. Section III describes our approach to determine the multifractal singularity spectrum of the DOS and the specific heat of the free electron gas in the Apollonian network. Numerical examples of the specific heat and a discussion of their temperature and band-filling dependence are then presented. The conclusions of this work are given in Sec. IV.

II. ELECTRON GAS IN THE APOLLONIAN NETWORK

We start with the definition of the Apollonian network in its simplest two-dimensional version by considering the problem of a space-filling packing of disks according to the ancient Greek mathematician Apollonius of Perga [31]. Three disks touch each other and the hole between them is filled by another disk that touches all the previous three, forming much smaller holes that are then filled again and so on. Connecting the centers of touching disks by lines, one obtains a network which gives a triangulation that physically corresponds to the force network of a dense granular packing. This network resembles the graphs introduced by Dodds [32] for the case of random packings and has also been used in the context of porous media [33]. Accordingly, at generation n $(n=0,1,2,\ldots)$ there are $m(k,n)=3^n,3^{n-1},3^{n-2},\ldots,3^2,3,1$, and 3 vertices with degree $k=3,3.2,3.2^2,\ldots,3.2^{n-1},3.2^n,2^{n+1}+1$, respectively, where the last number of vertices and degree correspond to the three corners, P_1, P_2, and P_3 (see Fig. 1).

We will consider an electron gas composed of N_e noninteracting electrons that can hop among the sites of an Apollonian network. We assume that hopping is only allowed between touching disks. In Fig. 1, we reproduce the first generations of the resulting network. As already mentioned, such a network has several important properties. In spite of being a deterministic network, it displays scale-free and small-world characteristics. In addition, such a complex network has no translational invariance and cannot be separated in interconnected sublattices.

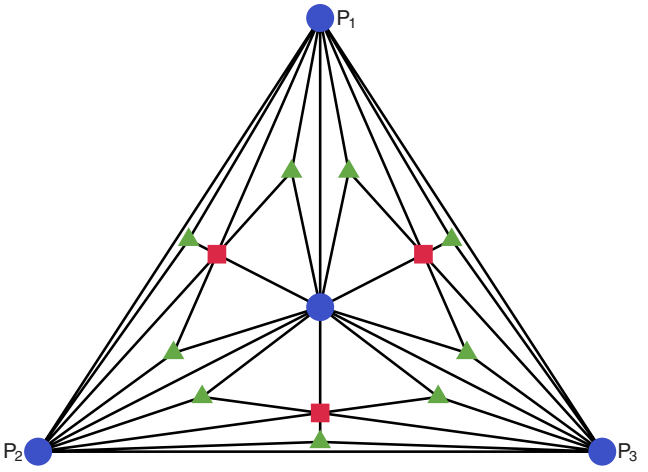

FIG. 1. (Color online) Second generation of the Apollonian network. P_1, P_2, and P_3 represent the corner sites. Different symbols refer to sites added at each new generation (central circle: $n=0$; squares: $n=1$; and triangles: $n=2$). The number of sites added in each generation is given by 3^n.

In order to obtain the eigenstates and energy spectrum for one particle restricted to hop among the sites of the above scale-free Apollonian network, we consider a tight-binding Hamiltonian written in the form

$$H = \epsilon \sum_i |i\rangle\langle i| + \sum_{(i,j)} t_{ij}|i\rangle\langle j|, \tag{1}$$

where $|i\rangle$ is a Wannier state localized at site i of the network. The hopping amplitudes will be taken as $t_{ij}=t$ whenever the pair of sites (i,j) represent the centers of touching disks of the Apollonian packing and $t_{ij}=0$ otherwise. The on-site potential energy is taken to be the same for all sites and will be set to $\epsilon=0$ hereafter without any loss of generality. The one-particle eigenstates can be expanded in the Wannier state basis as $|\Psi\rangle=\Sigma_i \phi_i|i\rangle$. Therefore the coefficients of the eigenstates expansion and the energy spectrum can be obtained from the set of coupled equations,

$$t\sum_j \phi_j = E\phi_i, \tag{2}$$

where the sites j are those connected with the ith site. The above set of equations can be numerically solved by direct diagonalization of the associated matrix for lattices with a finite number of generations. Recently, several spectral properties of this system were analyzed following this approach [21,34]. In particular, the localized and extended character of the energy eigenstates have been investigated, as well as their degeneracy degree associated with the $2\pi/3$ rotation symmetry of the Apollonian network [34]. Here, we are going to characterize the scaling behavior of the corresponding density of states and explore its influence on the thermodynamic behavior of the free-electron gas.

In Fig. 2, we display the integrated density of states obtained from a network with $n=8$ generations, which means a

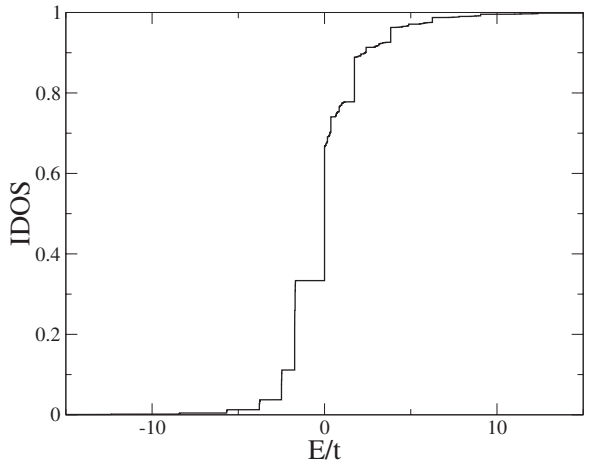

FIG. 2. Integrated density of states for an Apollonian network with $n=8$ generations. The vertical segments signal degenerated energy levels while the horizontal segments are associated with energy gaps. The largest degeneracy is at $E=0$ which supports $1/3$ of the one-particle states. Minibands are present in the upper half of the spectrum.

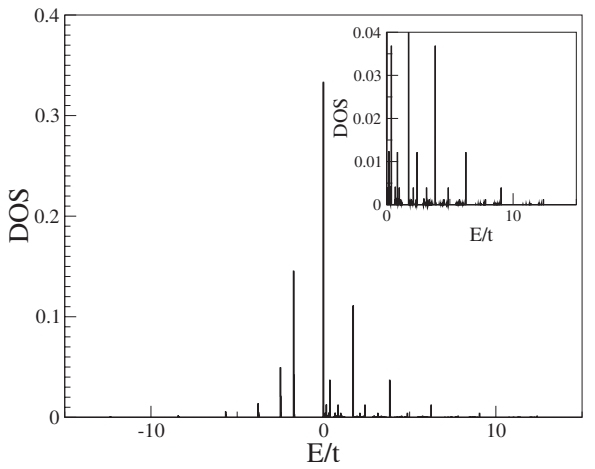

FIG. 3. Density of states representing the fraction of states located in small energy windows $\Delta E/t=10^{-2}$ for a $n=8$ Apollonian network. The first half of the energy spectrum is mainly composed of a discrete set of degenerated levels separated by gaps, while in the second half the minibands are visible. The presence of many scales of energy gaps and degeneracies suggests a fractal scaling. The inset is an amplification of the DOS showing the minibands above the band center.

total of $N=9844$ sites. The main characteristics of this energy spectrum, which correspond to the eigenvalues of the adjacency matrix of the Apollonian network, were reported in Ref. [21]. Some relevant aspects deserve to be pointed out. First, there are several degenerated energy levels. The most degenerated level is at $E/t=0$ accommodating $1/3$ of the total number of states. Additional degeneracies are also found as one approaches the bottom as well as the top of the energy spectrum with decreasing degrees. The spectrum also exhibits a set of energy gaps signaled by the horizontal segments of the integrated density of states. These energy gaps are well-defined at the first half of the energy spectrum which is mainly composed of a discrete set of degenerated energies. At the upper half of the spectrum, the intervals between degenerated energies are filled by minibands forming a continuum of states. However, the total number of states in these minibands represents only a small fraction of the total number of states which vanishes in the thermodynamic limit [21,34]. The above features become more apparent in Fig. 3 where we plot the density of states measured as the fraction of states within small energy windows $\Delta E=10^{-2}$. The asymmetric form of the density of states is a consequence of the absence of chiral symmetry of the Apollonian network, i.e., of the fact that this lattice cannot be decomposed into two independent sublattices with nonzero matrix elements connecting only sites of different sublattices. We also computed the density of states for lattices with a smaller number of generations in order to evaluate the finite-size corrections. These are mainly affecting the exponential tails with no relevant impact on the main features of the density of states.

III. MULTIFRACTAL SCALING ANALYSIS AND SPECIFIC HEAT

The presence of degeneracies and gaps at several energy scales suggests that the above density of states for the one-particle tight-binding Hamiltonian in an Apollonian network has a fractal-like scaling. In order to explore the asymptotic scaling behavior of the density of states, we consider it as representing a normalized measure giving the fraction of states within each energy window. Therefore the energy spectrum is split into N energy windows of the same size and the fraction of states within each window is considered as being a normalized measure $p_j(N)$. Actually, the spectrum of complex systems may exhibit multiscaling with independent power-law exponents governing the different moments of the probability distribution. Halsey *et al.* [35] introduced a formalism to characterize such multifractal measures. The formalism defines a generalized partition function $\chi_q(N)=\Sigma_{j=1}^{N}p_j^q$. In the $N\to\infty$ limit, the main contribution to $\chi_q(N)$ comes from a subset of all possible windows, whose number scales as $N_q\propto N^{f(q)}$. The content in each contributing box scales as $P_q\propto N^{-\alpha(q)}$. The multifractal measure is then characterized by the continuous function $f(\alpha)$ which reflects the different fractal dimensions of the subsets with singularity strength α.

There are several schemes in the literature to compute the spectrum of multifractal exponents. Here, we will use the one introduced by Chhabra and Jensen [36] conceived to characterize measures that arise from multiplicative processes with a uniform grid at the nth level of the process. It consists of determining the Hausdorff dimensions of a family of generalized normalized measures defined as

$$\mu_i(q,N)=\frac{p_i(N)^q}{\Sigma_{j=1}^{N}p_j(N)^q}. \tag{3}$$

The Hausdorff dimension of the asymptotic support of $\mu(q)$ is given by

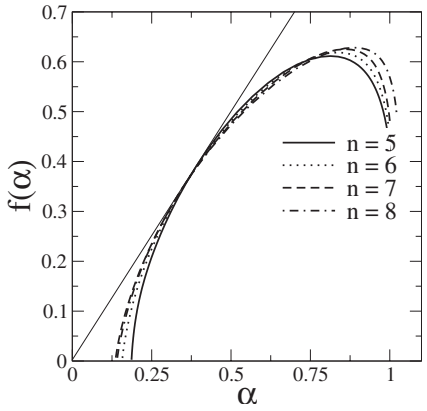

FIG. 4. Multifractal singularity spectrum of the density of states for one particle in Apollonian networks with $n=5$, 6, 7, and 8 generations. For computing the multifractal exponents, the energy spectrum was partitioned in N boxes, where N is the total number of sites for each generation. Finite-size corrections are mainly affecting the extremal segments of the singularity spectrum. The slight increase of the range of values for α for larger sizes confirms the multiscaling nature of the density of states in the thermodynamic limit.

$$f(q) = -\lim_{N\to\infty} \frac{1}{\ln N} \sum_{i=1}^{N} \mu_i(q,N) \ln \mu_i(q,N), \tag{4}$$

for which the average singularity strength can be evaluated as

$$\alpha(q) = -\lim_{N\to\infty} \frac{1}{\ln N} \sum_{i=1}^{N} \mu_i(q,N) \ln p_i(q,N). \tag{5}$$

Multifractal scaling ideas have been widely used to investigate a large class of complex systems, such as turbulent flow [37–39], dynamical systems [40–42], and phase transitions [43–45], among many others [46–48]. In order to evaluate the singularity spectrum $f(\alpha)$ of the density of states for one particle in the Apollonian network, we partitioned the energy spectrum of networks with a distinct number of generations. The number of windows was chosen to be equal to the total number of sites. In Fig. 4, we report the estimated singularity spectrum of networks with $n=5$, 6, 7, and 8 generations. Significant finite-size corrections are mainly present at the extremal regions of the singularity spectrum. These regions are associated with the extremal sets of the multifractal measures. However, the increasing range of values for α as the size of the network is increased confirms the multiscaling nature of the density of states in the thermodynamic limit. The maximum value of the fractal dimension $f_{max}<1$ is associated with the presence of gaps (regions of null measure) of many energy scales. The set of the measure with the minimal singularity strength α supports the regions with maximal probability. In the thermodynamic limit, it is dominated by the single degenerate level at $E=0$ which is consistent with a zero Hausdorff dimension for this set. On the other hand, the set with maximal singularity strength represents the boxes with minimal probability. In this case, these

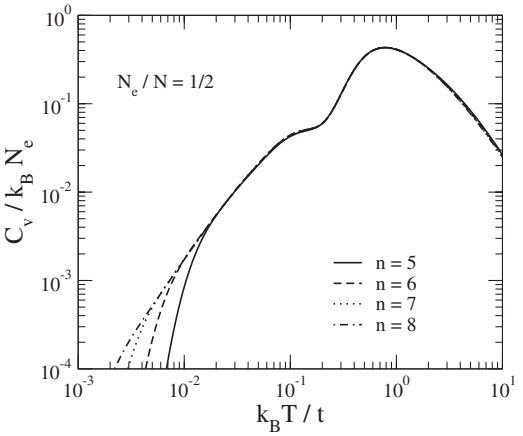

FIG. 5. Specific heat per electron as a function of temperature for the case of a half-filled band $N_e/N=1/2$. Apollonian networks with $n=5$, 6, 7, and 8 generations were considered. Finite-size corrections are only significant at very small temperatures. The high temperature decay $C_v \propto 1/T^2$ is typical of systems with a bounded energy spectrum. The anomaly observed as a strong deviation from the usual power-law low-temperature behavior reflects the existence of energy gaps near the Fermi energy.

are the boxes enclosing the continuum minibands and have a finite fractal dimension.

The thermodynamic behavior of an electron gas composed of N_e noninteracting electrons in an Apollonian network can be directly obtained from the above multifractal energy spectrum. According to the Fermi-Dirac statistics, the average occupation number of each energy state is given by

$$\langle n_i \rangle = \frac{1}{1+\exp[\beta(\epsilon_i - \mu)]}, \tag{6}$$

where $\beta=1/k_BT$ and μ is the chemical potential. Here, we are not including the spin degeneracy. An Apollonian network with n generations has $N=3+(3^{n+1}-1)/2$ sites. Therefore the chemical potential can be computed as a function of the temperature and the band filling N_e/N by imposing that $N_e=\Sigma_{i=1}^{N}\langle n_i\rangle$, from which $\mu(N_e/N,T)$ can be numerically extracted.

The specific heat of such electron gas at constant volume can be computed explicitly as $C_v=dU\ (N_e/N,T)/dT|_V$, where V is the volume of the system which is kept constant by fixing the number of generations of the Apollonian network. The average internal energy is expressed as $U(N_e/N,T)=\Sigma_i \epsilon_i \langle n_i\rangle$. It is straightforward to show that the specific heat can be put in the form

$$C_v/k_B = (\beta/2)^2 \left(\sum_i \epsilon_i^2 \cosh^{-2}[\beta(\epsilon_i-\mu)/2] - \frac{\{\Sigma_i \epsilon_i \cosh^{-2}[\beta(\epsilon_i-\mu)/2]\}^2}{\Sigma_i \cosh^{-2}[\beta(\epsilon_i-\mu)/2]} \right). \tag{7}$$

In Fig. 5, we show the specific heat for the case of half band filling $(N_e/N=1/2)$ as computed considering Apollonian networks with distinct generations. From these curves, we can evaluate the magnitude of the finite-size corrections

to the thermodynamic behavior present in our calculations. We can see clearly that for a network with $n=8$ generations, the finite-size corrections are very small for temperatures larger than $k_BT/t=10^{-3}$ and specific heat per particle as small as $C_v/N_e=10^{-4}k_B$. There are some features in the temperature dependence of the specific heat that deserve to be stressed. First, it presents a $1/T^2$ decay at high temperatures, as expected for systems with a bounded energy spectrum. Further, at low temperatures, it follows closely a power-law behavior, as usual for free-electron gases. There is a clear deviation from this behavior at a temperature of the order $k_BT/t=10^{-1}$. In order to understand this feature, one should notice that, at half filling, the Fermi energy is located exactly at the band center $E=0$ with this degenerated level partially filled. At very low temperatures, the electrons close to the Fermi energy are thermally excited to the miniband right above $E=0$ (see Fig. 3). However, this miniband supports only a very small fraction of electrons. After the initial thermal excitation, this miniband becomes fully occupied. This miniband and the degenerated states at $E=0$ are separated from the other allowed states by energy gaps. Therefore the system starts to lose its capacity to exchange energy with a thermal reservoir up to a temperature high enough to promote the electrons to the closest unoccupied energy states. It is important to mention that the specific heat of strongly correlated electrons interacting via a Hubbard Hamiltonian in the Apollonian network was recently analyzed [49]. At half filling, it was shown that a low-temperature peak emerges in the regime of strong interactions due to low-lying collective excitations. In the limit of vanishing Hubbard coupling, the specific heat exhibited a single peak, as the one here reported. However, the numerical procedure used to study strongly correlated electron systems limited the analysis based on the exact diagonalization of the Hamiltonian to a very small network encompassing only seven sites. Therefore the low temperature anomaly due to the structured character of the density of states, as well as its asymptotic power-law decay for very large networks, as it is shown in Fig. 5, could not be observed in Ref. [49].

The above anomaly on the specific heat becomes even more pronounced at smaller band fillings. In Fig. 6, we show the cases of $N_e/N=1/4$, $1/8$, and $1/16$. As the band filling decreases, the Fermi energy falls deeper in the fractal structure of the energy spectrum composed of degenerated levels separated by energy gaps. Therefore different energy scales associated with the fractal nature of the gaps emerge as a sequence of oscillations in the specific heat. In the limit of very small band fillings, the Fermi-Dirac statistics become equivalent to the classical Maxwell-Boltzmann statistics. In this case, the specific heat of systems with a fractal energy spectrum develops log-periodic oscillations in the specific heat, a trend indeed observed in Fig. 6.

The absence of chiral, and consequently, of electron-hole symmetry in the Apollonian network can be observed in the temperature dependence of the specific heat. In Fig. 7, we plot the specific heat per hole considering band fillings of $N_e/N=3/4$, $7/8$, and $15/16$ which are complementary of those depicted in the previous figure. In these cases, the Fermi-energy falls in a region where the degenerated energy levels are separated by minibands. The presence of minibands smoothes the oscillations in the temperature dependence of the specific heat. Further, as we approach the full band regime, the low temperature specific heat of holes becomes much smaller than that for electrons once the degeneracies are smaller at the top than at the bottom of the energy band.

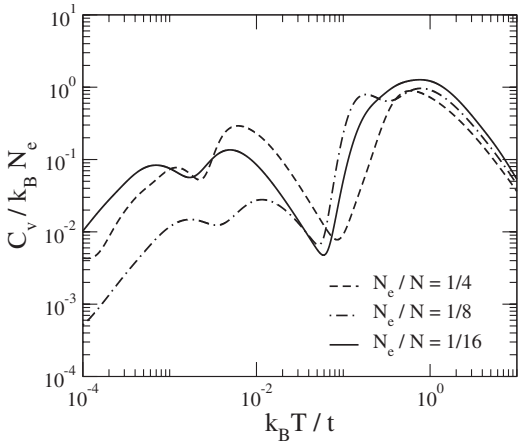

FIG. 6. Specific heat per electron as a function of temperature in an Apollonian network with $n=8$ generations and band fillings $N_e/N=1/4$, $1/8$, and $1/16$. The oscillations in the specific heat are associated with the increasing number of scales of energy gaps and degeneracies as one approaches the bottom of the band. In the limit of $N_e/N\rightarrow 0$ the specific heat starts to develop log-periodic oscillations, as expected for classical systems with a fractal energy spectrum.

IV. CONCLUSIONS

In summary, we studied the free-electron gas in an Apollonian network. We have shown that the scale-free nature of

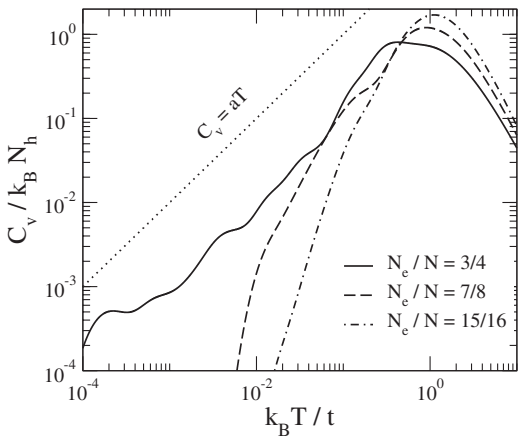

FIG. 7. Specific heat per hole ($N_h=N-N_e$) as a function of temperature in an Apollonian network with $n=8$ generations and band fillings $N_e/N=3/4$, $7/8$, and $15/16$, complementary to those depicted in Fig. 6. The absence of electron-hole symmetry is clearly evident. The presence of minibands at the upper half of the energy spectrum smoothes the oscillations in the specific heat. The specific heat per hole for large band fillings becomes smaller than the corresponding specific heat per electron at low fillings due to the lower degree of degeneracy at the top of the energy spectrum.

the network leads to a multifractal energy spectrum that presents degeneracies, gaps, and minibands of several scales. The absence of chiral symmetry of the lattice implies an asymmetry of the density of states, leading to distinct properties associated with electrons and holes. We reported the multifractal singularity spectrum of the density of states and showed that, while the region containing the largest density of states is of null measure with zero fractal dimension, the minibands are distributed on a fractal support. We also showed that the fractal structure of the energy spectrum has strong signatures in the thermodynamic behavior of the Apollonian electron gas. Logarithmic oscillations in the temperature dependence of the specific heat reveals the existence of several energy scales in the underlying spectrum. These oscillations are more pronounced at low band fillings because the lower-half of the energy spectrum has a more sharply defined fractal sequence of energy levels. At the upper half of the spectrum, the presence of minibands suppresses the specific heat oscillations, giving a clear thermodynamic evidence of the absence of electron-hole symmetry. It would be interesting to investigate if other Hamiltonian systems defined in scale-free lattices would have a similar multifractal energy spectrum as well as its thermodynamic signatures. In particular, the study of collective excitations, such as phonons and magnons, in scale-free lattices would contribute to a more complete scenario for the understanding of the solid state properties of such complex structures. We hope the present results can stimulate further works along these directions.

ACKNOWLEDGMENTS

This work was financially supported by CNPq, Rede Nanobioestruturas, CAPES, FINEP (Brazilian research agencies), FAPEAL (Alagoas State agency), and FUNCAP (Ceará State Agency).

[1] D. Shechtman, I. Blech, D. Gratias, and J. W. Cahn, Phys. Rev. Lett. **53**, 1951 (1984).
[2] J. Bellisard, A. Bovier, and J.-M. Ghez, Commun. Math. Phys. **135**, 379 (1991); A. Bovier and J.-M. Ghez, *ibid.* **158**, 45 (1993).
[3] P. A. Lee and T. V. Ramakrishnan, Rev. Mod. Phys. **57**, 287 (1985).
[4] J. B. Sokolof, Phys. Rep. **126**, 189 (1985).
[5] E. L. Albuquerque and M. G. Cottam, Phys. Rep. **376**, 225 (2003).
[6] R. Albert and A.-L. Barabási, Rev. Mod. Phys. **74**, 47 (2002).
[7] R. Sharan and T. Ideker, Nat. Biotechnol. **24**, 427 (2006).
[8] S. Wassermann and K. Faust, *Social Network Analysis* (Cambridge University Press, Cambridge, England, 1994).
[9] A.-L. Barabási and R. Albert, Science **286**, 509 (1999).
[10] R. Cohen, K. Erez, D. ben-Avraham, and S. Havlin, Phys. Rev. Lett. **85**, 4626 (2000).
[11] R. Cohen, K. Erez, D. ben-Avraham, and S. Havlin, Phys. Rev. Lett. **86**, 3682 (2001).
[12] A. A. Moreira, J. S. Andrade, and L. A. Nunes Amaral, Phys. Rev. Lett. **89**, 268703 (2002).
[13] A. F. Rozenfeld, R. Cohen, D. ben-Avraham, and S. Havlin, Phys. Rev. Lett. **89**, 218701 (2002).
[14] J. Quintanilla and V. L. Campo, Phys. Rev. B **75**, 144204 (2007).
[15] L. K. Gallos, C. Song, and H. A. Makse, Phys. Rev. Lett. **100**, 248701 (2008).
[16] S. Jung, S. Kim, and B. Kahng, Phys. Rev. E **65**, 056101 (2002).
[17] S. N. Dorogovtsev, A. V. Goltsev, and J. F. F. Mendes, Phys. Rev. E **65**, 066122 (2002).
[18] J. S. Andrade, H. J. Herrmann, R. F. S. Andrade, and L. R. da Silva, Phys. Rev. Lett. **94**, 018702 (2005).
[19] J. P. K. Doye and C. P. Massen, Phys. Rev. E **71**, 016128 (2005).
[20] D. J. B. Soares, J. S. Andrade, H. J. Herrmann, and L. R. da Silva, Int. J. Mod. Phys. C **17**, 1219 (2006).
[21] R. F. S. Andrade and J. G. V. Miranda, Physica A **356**, 1 (2005).
[22] J. P. K. Doye and C. P. Massen, J. Chem. Phys. **122**, 084105 (2005).
[23] A. A. Moreira, D. R. Paula, R. N. Costa Filho, and J. S. Andrade, Phys. Rev. E **73**, 065101(R) (2006).
[24] C. Tsallis, L. R. da Silva, R. S. Mendes, R. O. Vallejos, and A. M. Mariz, Phys. Rev. E **56**, R4922 (1997).
[25] R. O. Vallejos, R. S. Mendes, L. R. da Silva, and C. Tsallis, Phys. Rev. E **58**, 1346 (1998).
[26] L. R. da Silva, R. O. Vallejos, C. Tsallis, R. S. Mendes, and S. Roux, Phys. Rev. E **64**, 011104 (2001).
[27] I. N. de Oliveira, M. L. Lyra, and E. L. Albuquerque, Physica A **343**, 424 (2004).
[28] I. N. de Oliveira, M. L. Lyra, E. L. Albuquerque, and L. S. da Silva, J. Phys.: Condens. Matter **17**, 499 (2005).
[29] P. W. Mauriz, E. L. Albuquerque, and M. S. Vasconcelos, Phys. Rev. B **63**, 184203 (2001); Physica A **294**, 403 (2001).
[30] C. G. Bezerra, E. L. Albuquerque, A. M. Mariz, L. R. da Silva, and C. Tsallis, Physica A **294**, 415 (2001); C. G. Bezerra, E. L. Albuquerque, and M. G. Cottam, *ibid.* **301**, 341 (2001).
[31] D. W. Boyd, Can. J. Math. **25**, 303 (1973).
[32] J. A. Dodds, J. Colloid Interface Sci. **77**, 317 (1980).
[33] P. M. Adler, Int. J. Multiphase Flow **11**, 91 (1985).
[34] A. L. Cardoso, R. F. S. Andrade, and A. M. C. Souza, Phys. Rev. B **78**, 214202 (2008).
[35] T. C. Halsey, M. H. Jensen, L. P. Kadanoff, I. Procaccia, and B. I. Shraiman, Phys. Rev. A **33**, 1141 (1986).
[36] A. Chhabra and R. V. Jensen, Phys. Rev. Lett. **62**, 1327 (1989).
[37] J. F. Muzy, E. Bacry, and A. Arneodo, Phys. Rev. Lett. **67**, 3515 (1991).
[38] P. Kestener and A. Arneodo, Phys. Rev. Lett. **91**, 194501 (2003).
[39] L. Biferale, G. Boffetta, A. Celani, B. J. Devenish, A. Lanotte, and F. Toschi, Phys. Rev. Lett. **93**, 064502 (2004).
[40] V. Afraimovich and G. M. Zaslavsky, Phys. Rev. E **55**, 5418

(1997).
[41] C. R. da Silva, H. R. da Cruz, and M. L. Lyra, Braz. J. Phys. **29**, 144 (1999).
[42] N. Hadyn, J. Luevano, G. Mantica, and S. Vaienti, Phys. Rev. Lett. **88**, 224502 (2002).
[43] M. Schreiber and H. Grussbach, Phys. Rev. Lett. **67**, 607 (1991).
[44] A. D. Mirlin, Y. V. Fyodorov, A. Mildenberger, and F. Evers, Phys. Rev. Lett. **97**, 046803 (2006).
[45] C. Monthus and T. Garel, Phys. Rev. E **76**, 021114 (2007).
[46] H. E. Stanley, L. A. N. Amaral, A. L. Goldberger, S. Havlin, P. C. Ivanov, and C. K. Peng, Physica A **270**, 309 (1999).
[47] A. Turiel and C. J. Perez-Vicente, Physica A **322**, 629 (2003).
[48] J. Ozik, B. R. Hunt, and E. Ott, Phys. Rev. E **72**, 046213 (2005).
[49] A. M. C. Souza and H. Herrmann, Phys. Rev. B **75**, 054412 (2007).